ADVANCED BEAM COUPLING IMPEDANCE MODELING FOR LHC AND HL-LHC APPLICATIONS*

C. Zannini†, C. Antuono, E. de la Fuente Garcia, G. Rumolo, B. Salvant, L. Sito, J. Sonpar
CERN, Geneva, Switzerland

Abstract

Accurate beam coupling impedance modeling is essential for predicting collective effects and ensuring stable high-intensity operation in the LHC and its High-Luminosity upgrade. Operational experience has shown that even small mechanical details can have a significant impact on the impedance of accelerator components, potentially leading to performance degradation or hardware failure. In addition, impedance sources are not static: beam-induced heating and the resulting mechanical stresses can drive gradual geometric changes, such as loss of electrical contact or deformation of shielding elements, thus modifying the impedance during operation. In this work, we present recent advancements in high-fidelity impedance modeling and demonstrate their relevance through representative case studies in the LHC. These examples show how improved modeling, combined with beam-based diagnostics, provides critical input for operational strategies and supports informed design and optimization of components in view of the challenging HL-LHC requirements.

INTRODUCTION

Accurate impedance modeling is a key ingredient for understanding beam stability and power deposition in the LHC and HL-LHC. Experience from operation has demonstrated that seemingly minor mechanical details, such as RF fingers or spring contacts, can significantly impact impedance and lead to measurable beam-induced heating.

Moreover, impedance is not a static property. Thermal loads and mechanical stresses can induce progressive geometric changes, such as loss of electrical contact or deformation of shielding structures, leading to a dynamic evolution of the impedance during operation.

These observations motivate the development of high-fidelity modeling approaches capable of capturing both detailed geometrical features and their evolution under realistic conditions.

Small-scale geometric features can significantly influence the impedance response and local power deposition, as demonstrated by the failure of an LHC warm vacuum module. This failure occurred in 2023 [1] and was attributed to localized heating of a tension spring used to ensure electrical contact between the fingers and the transition tube (see Fig. 1).

Advanced electromagnetic modeling enabled a detailed understanding of the impedance mechanism responsible for the failure. Beam-induced localized power deposition on the spring was identified, arising from beam offset and the asymmetric distribution of the fingers, which led to the observed localized heating. The estimated power levels were found to be consistent with the observed failure in the presence of degraded finger contact, explaining why the issue occurred only in a limited number of modules. Figure 2 illustrates the localized heating predicted by electromagnetic simulations, in agreement with the spring damage observed in 2023 [1]. This example highlights how geometric details can lead to strong field concentration and significant power deposition. Such effects are often not captured by simplified models, yet they are critical for understanding failure mechanisms.

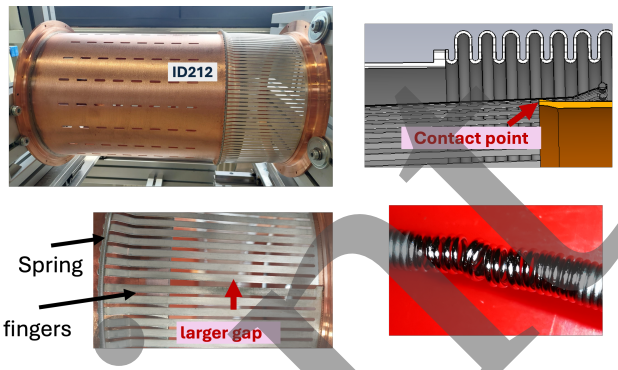

Figure 1: Example of spring contact geometry used in impedance simulations for an ID212 mm module. The top-left picture shows the transition tube, contact fingers, and the spring ensuring electrical contact between them. The top-right picture presents a detailed 3D view of the region between the transition tube and the fingers, which provides impedance shielding of the bellows (shown in gray). The bottom-left picture highlights the non-uniform finger spacing, while the bottom-right picture shows a locally burnt section of the spring.

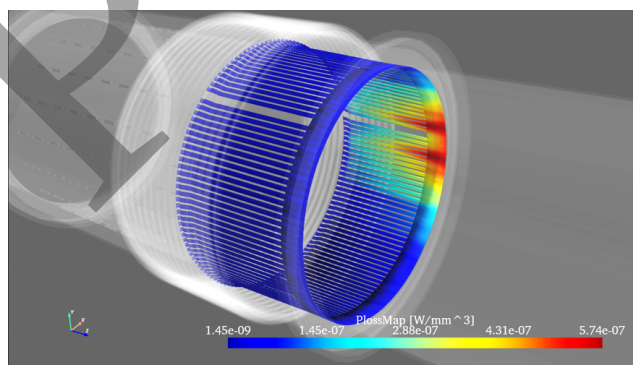

Figure 2: Beam induced power deposition on the ID212 module, highlighting localized heating regions.

* Research supported by the HL-LHC project
† carlo.zannini@cern.ch

ADVANCED IMPEDANCE MODELING METHODOLOGY

To capture these effects, advanced modeling approaches are required, combining high-resolution electromagnetic simulations, detailed geometrical representation, realistic material properties and coupling with thermal and mechanical effects. Such models enable a deeper understanding of impedance-driven mechanisms and allow linking electromagnetic fields to thermal loads and mechanical response. This approach is particularly important for identifying critical regions where small geometrical deviations can trigger large beam coupling impedance variations. Two examples are given in the following subsections.

Case Study 1: Understanding VMSIO Failure

An illustrative example is provided by the VMSIO failure scenario observed during the 2025 run, where non-ideal contact between the fingers and the transition tube significantly altered the beam coupling impedance. This led to plastic deformation of the spring, resulting in the loss or degradation of electrical contact. The configuration evolved during operation as the spring progressively lost its ability to maintain proper contact. Consequently, beam-induced heating and the associated structural deformation drove a continuous evolution of the beam coupling impedance throughout the run. This evolution could lead to more or less favorable conditions, ultimately determining whether operation remained stable or became unfeasible at a given beam intensity.

Figure 3 shows the non-conformal geometry reconstructed following the identification of the issue from X-ray analysis. The mechanism leading to impedance evolution along the run is illustrated in Fig. 4, which depicts a feedback loop where beam-induced heating modifies the geometry, thereby altering the impedance and further affecting power deposition. As an example of this mechanism, Fig. 5 shows the temperature evolution under identical beam parameters, clearly indicating an ongoing change in the impedance. A few weeks later, the temperature exhibited an opposite trend (increase) following a small intensity step, which acted as a perturbation to a previously stable system. Quantitative impedance assessments of the modified VMSIO geometry were used to guide beam intensity operational constraints during the 2025 run [2, 3].

Case Study 2: TCLD Beam-Induced Sparking Mitigation

The TCLD provides an example where advanced modeling supports design optimization and mitigation strategies [4, 5]. Since 2022, beam observations in the LHC have revealed a significant increase in vacuum activity associated with the TCLD, with pressure spikes observed when changing beam configurations, particularly filling patterns. This indicated a sensitivity to the beam spectral content and a behaviour compatible with sparking caused by the excitation of different regions of the device [6]. A conditioning effect over time was also observed for the same type of beam.

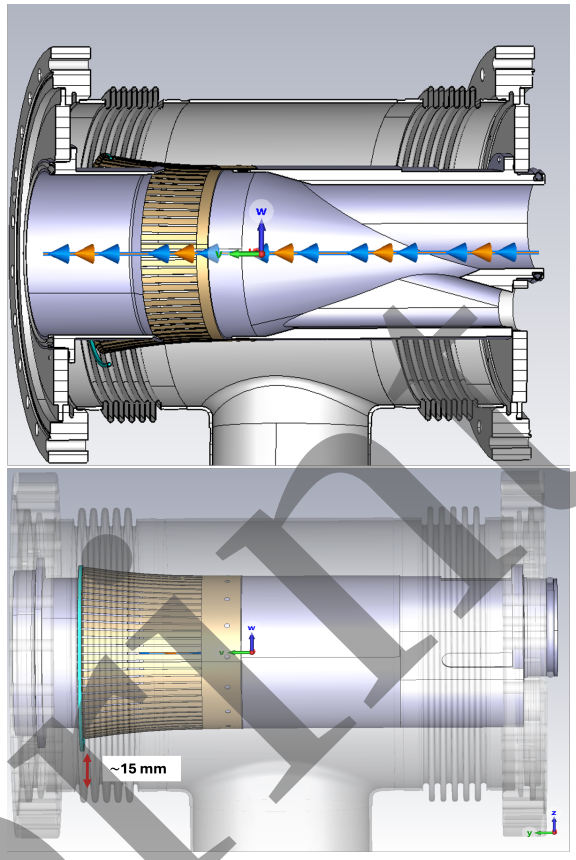

Figure 3: Top: cut view of the 3D model of the VMSIO used in CST simulations, with the fingers shown in yellow and the beam path indicated by arrows. Bottom: 3D model showing the elongated spring (light blue), located at an estimated distance of 15 mm from the bellows.

However, beam observations in 2025 showed an increase in vacuum levels during the first fills with 1.7×10^{11} protons per bunch, suggesting a possible contribution from beam-induced heating. These observations triggered a dedicated impedance study, supported by previous X-ray inspections of the installed TCLD, which revealed a specific RF-finger configuration, as shown in Fig. 6. This configuration was reproduced in detailed CST electromagnetic simulations [7], which showed that bent RF fingers can enhance resonant modes, increasing their impact and therefore the risk of beam-induced heating or sparking. These complex simulations predicted a reduction of impedance resonances for smaller collimator gaps, as illustrated in Fig. 7. This trend was experimentally confirmed by bench impedance measurements, where a progressive suppression of resonances was observed for different half-gap apertures, ranging from approximately 22 mm to 10 mm. The measurements confirmed the mitigation effect, while also enabling benchmarking of the impedance model and visually verifying similar RF-finger configurations in the spare TCLD devices.

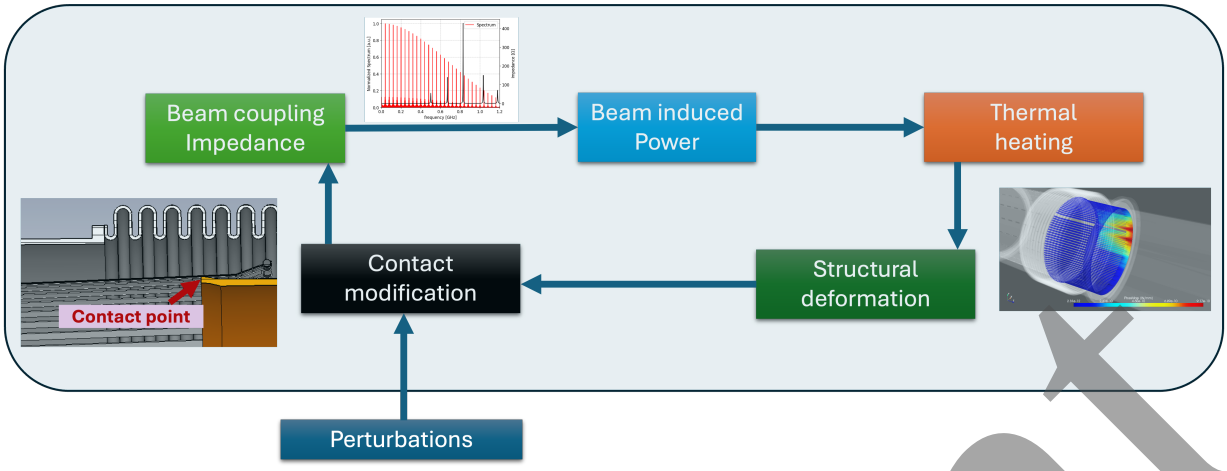

Figure 4: Illustration of the feedback mechanism driving impedance evolution: beam-induced heating modifies the geometry, which alters the beam coupling impedance and, in turn, changes the power deposition, potentially leading to further heating and deformation.

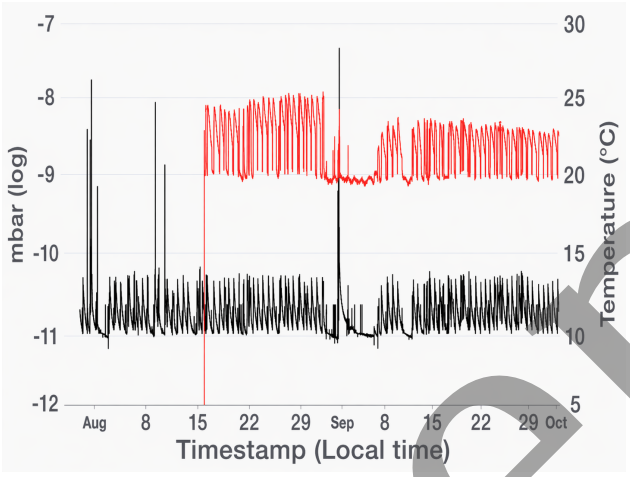

Figure 5: Measured pressure (black, left axis) and temperature (red, right axis) evolution under nominally identical beam conditions. The most pronounced pressure spike is followed by a decrease in temperature, indicating a transition to a different regime, likely associated with a modification of the beam coupling impedance.

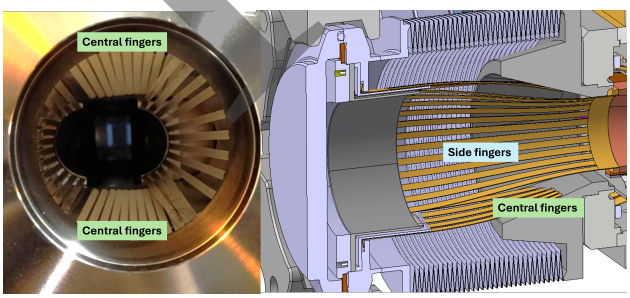

Figure 6: Pictures of TCLD RF fingers distribution of a spare device (left). TCLD 3D CAD geometry used in CST simulations for impedance assessment.

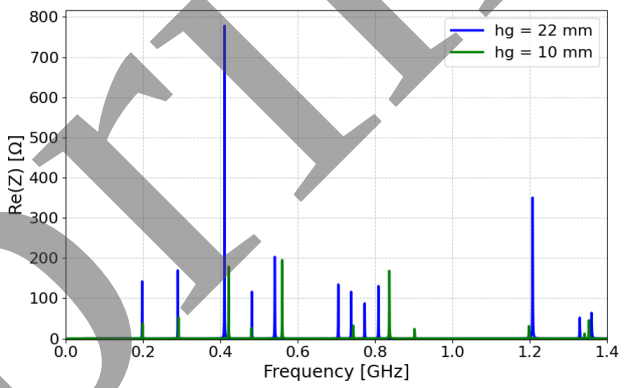

Figure 7: Comparison of the beam coupling impedance obtained for different gap configurations.

Although the exact in-machine configuration of the fingers remains uncertain, the combined impedance approach based on simulations and measurements provides a robust tool to guide and support operational decisions. In fact, these results motivated the reduction of the TCLD gap for the 2026 run as an effective mitigation strategy to minimize impedance-driven effects such as beam-induced heating or sparking. The adopted strategy appears to have led to a significant reduction in vacuum activity in the early phase of the run, despite the increased bunch intensity.

CONCLUSION

Advanced impedance modeling is essential to capture the impact of small mechanical details and their evolution under beam-induced effects. The presented case studies demonstrate that high-fidelity simulations, combined with beam-based diagnostics, provide a powerful tool to understand failure mechanisms and guide mitigation strategies.

These capabilities are particularly relevant for the HL-LHC, where tighter margins and higher beam intensities require accurate and predictive impedance models.

REFERENCES

[1] C. Antuono *et al.*, "Impact of high-intensity lhc beam operation on warm vacuum modules", *Phys. Rev. Accel. Beams*, vol. 28, p. 041001, 2025. doi:10.1103/PhysRevAccelBeams.28.041001

[2] C. Zannini *et al.*, "Estimation of power levels on rf fingers in the vmsio.6l2.b", CERN, Presentation at the 107th Impedance Working Group (IWG) meeting, CERN, 2025. https://indico.cern.ch/event/1582575/contributions/6669808/attachments/3127129/5546883/ppt_VSMIO.6L2_LBOC_vIWG.pdf

[3] C. Zannini and C. Antuono, "Impedance considerations on the VMSIO.6L2.B failure", Presentation at the LHC Machine Committee (LMC), CERN, 2026, https://lmc-public.web.cern.ch/node/605146,

[4] C. Antuono, "TCLD impedance studies", 2024. https://indico.cern.ch/event/1607306/contributions/6772182/attachments/3167927/5630581/TCLD_5_11_LMC_CA.pdf

[5] C. Antuono, "TCLD 5.11 Status and Outlook", 2024, https://indico.cern.ch/event/1609688/,

[6] C. Zannini, "ZS beam-induced sparking", Presentation at the 173rd HSC Meeting, CERN, 2019, https://indico.cern.ch/event/807899/contributions/3362764/attachments/1817273/2971081/ZS_beam_induced_sparking.pdf,

[7] Cst website, http://www.cst.com/